Electrical bistability in a xanthene class molecule: Conduction mechanisms

Arup K. Rath, Satyajit Sahu, and Amlan J. Pal

Citation: Appl. Phys. Lett. **89**, 142110 (2006); doi: 10.1063/1.2358946
View online: http://dx.doi.org/10.1063/1.2358946
View Table of Contents: http://apl.aip.org/resource/1/APPLAB/v89/i14
Published by the AIP Publishing LLC.

Electrical bistability in a xanthene class molecule: Conduction mechanisms

Arup K. Rath, Satyajit Sahu, and Amlan J. Pal[a)]
Department of Solid State Physics, Indian Association for the Cultivation of Science, Jadavpur, Kolkata 700032, India

(Received 8 July 2006; accepted 23 August 2006; published online 4 October 2006)

The author study conduction mechanism in two conducting states of a bistable device at 10–300 K range. They find that in the electrical bistable devices, electrical switching is associated with a change in the conduction mechanism. Device current in the low-conducting state follows an injection-limited mechanism. The current in the high-conducting state conforms a bulk-dominated mechanism, namely, space-charge limited conduction with an exponential distribution of traps. The bistability has an associated memory phenomenon. The devices exhibit read-only and random-access memory applications for several hours. © *2006 American Institute of Physics*. [DOI: 10.1063/1.2358946]

Memory phenomenon in organic molecules[1–6] is based on electrical bistability of the materials. The bistability is generally due to a change in conformation of the molecules,[7,8] electroreduction,[4,8–11] or polaron formation.[12] When the bistability is stable and sustainable without any bias, it is referred to as memory switching[3,4,11,13] (as opposed to threshold switching,[14,15] where a bias is needed to retain the high-conducting state). Molecules that exhibit such a bistability are considered for memory applications.[3,4]

In the light of two conducting states at a bias, it would be worthwhile to study the conduction mechanisms involved in the high- and low-conducting states. In metal/organic/metal structures, injection-dominated and bulk-dominated mechanisms are considered to explain current-voltage (*I-V*) characteristics.[16–19] The injection-dominated mechanisms were temperature-independent tunneling and temperature-dependent thermionic emission. With respect to bulk-dominated mechanisms, Ohmic conduction, space-charge limited conduction (SCLC), and SCLC with an exponential distribution of traps are considered. In this letter, we have studied different conduction mechanisms involved in electrically bistable devices.

Most of the biplanar molecules in xanthene class exhibit electrical bistability.[4] In the present work, we chose erythrosin B (inset of Fig. 1). Due to the presence of alkoxide and carboxylate moieties, the molecule can be deposited via layer-by-layer (LbL) electrostatic assembly with a suitable polycation, namely, poly(allylamine hydrochloride) (PAH). Both the materials were purchased from Aldrich Chemical Co. LbL films of erythrosin B with PAH were deposited following standard procedure.[8] The films were dried in a vacuum oven (10^{-3}Torr, 100 °C) for 6 h. Aluminum (Al) was thermally evaporated in vacuum on top of the erythrosin B films to complete device fabrication. Active area of each of the devices was 5.5 mm^2.

To study *I-V* characteristics at fixed temperatures, devices were kept in a cryostat (Janis CCS 150 closed cycle refrigerator). Temperature of the device structure was controlled by a LakeShore 331 temperature controller. *I-V* characteristics were recorded with a Yokogawa 7651 programmable dc source and a Keithley 486 picoammeter. Bias was applied to the indium tin oxide (ITO) electrode with respect to the Al.

I-V characteristics of devices based on 10 and 15 bilayers of erythrosin B for two voltage-sweep directions are shown in Fig. 1. The figure shows that the magnitude of current switches to a high value at around −2.2 V during the sweep from a positive voltage. During the sweep to a positive bias, the magnitude shows a sharp drop at around 2.6 V. In the scan from a negative voltage, magnitude of current at any bias is much higher as compared to that during the sweep from a positive voltage. In other words, current at a particular bias depends on the direction of voltage sweep. Magnitude of current for both high- and low-conducting states is expectedly higher in a ten-layer device as compared to the respective ones of a 15-layer device.

Threshold voltage (V_{th}), the bias at which switching to a high-conducting state occurs, does not depend of the thickness of the films. This shows that the switching is a voltage-driven process. In these molecules, due to the electron-accepting functional groups (iodine, in this case), conductivity of pristine material is in general low. Electroreduction, along with conformation change, results in increased conjugation in these biplanar molecules. Hopping process through the conjugated moieties leads to the high-conducting state of the device.

The switching between the two states is reversible in nature and occurs in cycles. Figure 2 shows *I-V* characteristics of a device in three consecutive loops. The figure, plotted in log-linear scale, shows that when bias is applied in a loop, the electrochemical reaction processes also cycle reversibly resulting in reproducible *I-V* characteristics. The figure further shows that the on/off ratio, the ratio between current

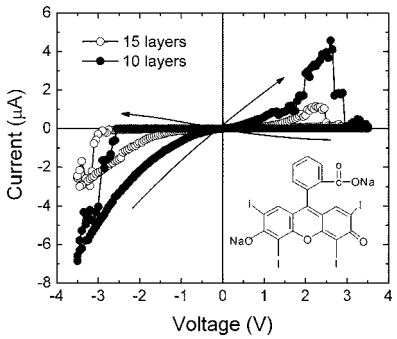

FIG. 1. *I-V* characteristics of devices based on 10 and 15 bilayers of erythrosin B at room temperature in two voltage-sweep directions (as shown by arrows). Inset shows the molecular structure of erythrosin B.

[a)]Electronic mail: sspajp@iacs.res.in

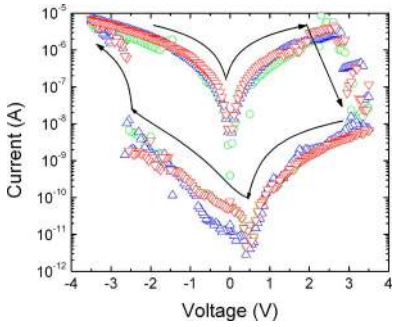

FIG. 2. (Color online) *I-V* characteristics of a device based on ten bilayers of erythrosin B at room temperature in three voltage loops. Arrows show the direction of voltage sweep.

values at a voltage during the two sweeps, is mostly voltage independent and remains invariant from a loop to the other. The ratio ranges up to 3000 at −1.0 V. Such a high value, especially at room temperature, is itself of interest due to its possible application as memory elements.

In Figs. 3(a) and 3(b), we present performance of a device for read-only and random-access memory, ROM and RAM, respectively, applications. For ROM applications, a suitable voltage pulse induces a state before probing it continuously. Figure 3(a) shows the magnitude of current under probe voltage after the low- and high-states are induced separately. The figure shows that the magnitude depends on the preceding pulse. The large difference in current in probing the two states shows ROM application for several hours. For RAM applications, we cycled the device between the two states and measured the current under the same probe voltage. In effect, the device underwent a "write-read-erase-read" sequence. Such a voltage sequence and corresponding current are plotted in Fig. 3(b). The figure shows that the magnitude of current under "read" voltage after "write" pulse is much higher than that after the "erase" pulse. The difference in current in probing the two states shows RAM application of the device for many cycles.

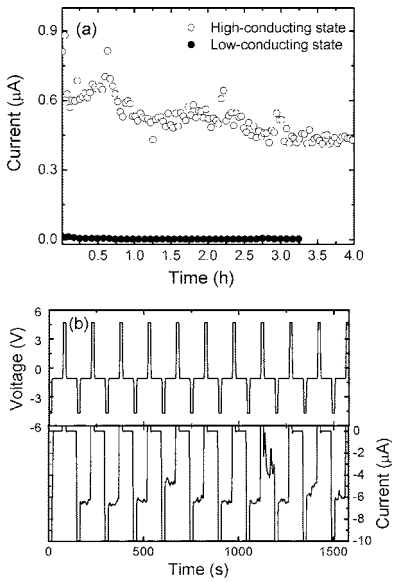

FIG. 3. (a) ROM and (b) RAM applications of a device based on ten bilayers of erythrosin B. In (a), the high- and low-conducting states were induced by −3.5 and 3.5 V pulses (width=20 s), respectively. The states were probed by −0.9 V pulse of 2 s width (duty cycle=50%). Magnitude of current is plotted in the figure. In (b), bias sequence for "write-read-erase-read" cycle and corresponding current are plotted in the two panels. The measurements were carried out at room temperature.

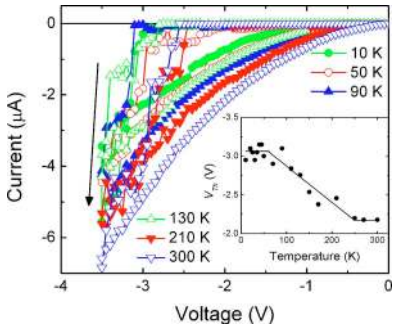

FIG. 4. (Color online) Temperature dependence of *I-V* characteristics of a device based on ten bilayers of erythrosin B in two voltage-sweep directions. Reverse bias section of the characteristics is shown. The arrow shows the direction of conductance switching in the device at all temperatures. Inset shows temperature dependence of threshold voltage V_{th}. The line is to guide the eyes.

To study transport mechanism in the two states, we have recorded *I-V* characteristics at 19 different temperatures down to 10 K. At each temperature, we recorded the characteristics in the two voltage-sweep directions (Fig. 4). The device shows bistability at all temperatures. Magnitude of V_{th}, which is a measure of the bias at which conductivity of the molecules switches to a high state, increases with decrease in temperature (inset of Fig. 4). Increase in V_{th} at low temperature can hence be due to increase in the magnitude of reduction potential with decrease in temperature. While magnitude of current for the high states decreases with decrease in temperature, the one for the low state shows a little temperature dependence.

The characteristics of the low state can be fitted to an injection-dominated mechanism. As per thermionic emission mechanism, the current density is given by[20]

$$J = A^* T^2 \exp[-q(\phi_B - \sqrt{qE/4\pi\varepsilon})/kT],$$

where A^* is Richardson's constant, T is the absolute temperature, q is the magnitude of electronic charge, ϕ_B is the barrier height, E is electric field, ε is dielectric permittivity, and k is Boltzmann's constant. Figure 5(a)—plots of $\ln(I)$ vs $\ln(V^{1/2})$ at different temperatures—shows linear fit in the higher bias region. The slope of the plots yields dielectric constant of 3 at room temperature, which is in agreement to the values obtained from impedance spectroscopy.[21] This shows validity of thermionic emission model in the low-conducting state of the device. In the analysis of the *I-V* characteristics, we have taken built-in potential (V_{bi}) into account. The difference between the metal work functions V_{bi} perturbs the field across the device.

Current in the high-conducting state, on the other hand, did not fit to injection-dominated mechanisms. We could fit them to a bulk-dominated mechanism, namely, SCLC with an exponential distribution of traps.[22] Space-charge limited current, which dominates when the concentration of injected carriers exceeds the carriers produced by thermal excitation, requires Ohmic contact with the electrode. Ohmic contact is a possibility in the high-conducting state due to decrease in band gap of erythrosin B upon electroreduction. A decrease in the band gap is generally evident in case of polaron formation in these materials. Moreover, electronic absorption spectroscopy of erythrosin B solution shows that the absorp-

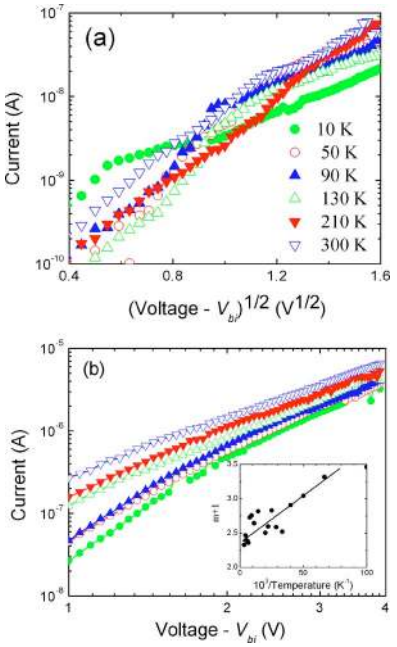

FIG. 5. (Color online) Fitting of (a) low-conducting and (b) high-conducting state currents following thermionic emission model and SCLC with exponential distribution of traps, respectively. Inset of (b) shows variation of the slope of $\ln(I)$-$\ln(V-V_{\mathrm{bi}})$ plot, $m+1$, vs inverse of temperature. The line is the best fit to the experimental points.

tion maximum shifts towards a low energy upon reduction. The process is reversible exhibiting a blueshift in absorption maximum upon oxidation. Here the decrease in the band gap must be associated with a decrease in lowest unoccupied molecular orbital (LUMO) level or increase in highest occupied molecular orbital (HOMO) level. Calculation on single molecules evidenced change of both the levels.[23] Such a change of the HOMO and LUMO levels leads to decrease in the barrier heights with the metal electrodes and results in Ohmic contact with them.

According to the SCLC mechanism with traps having energies distributed exponentially over the band gap, current density is given by[22]

$$J = K\frac{V^{m+1}}{d^{2m+1}},$$

where d is sample thickness and K is determined by ε, hole mobility (μ_p), density of states in the HOMO level (N_{HOMO}), total trap density (N_t), and m. Here m generally relates to characteristic temperature of the exponential trap distribution (T_t) as $m=T_t/T$, where T is the temperature at which I-V characteristics were recorded.

The I-V characteristics of the high-conducting state at different temperatures are presented in Fig. 5(b). At lower voltages, where concentration of injected carriers is low, the I-V plots fit to Ohm's law. In the intermediate and high voltage regions, the plots fit to the bulk-dominated mechanism. The plots tend to meet at a critical voltage V_c, where all the traps are filled. Beyond the critical bias, temperature-independent and trap-free space-charge limited current should flow.[24]

To validate applicability of the mechanism, we have determined the slope of $\ln(I)$ vs $\ln(V-V_{\mathrm{bi}})$ plots. A plot of the slope $m+1$ versus inverse of temperature, as presented in the inset of Fig. 5(b), fits to a straight line. The fitting confirms that space-charge dominated conduction mechanism with an exponential distribution of traps is applicable to the high state of the device. The value of m is much lower than that calculated commonly in organic and polymeric light-emitting devices (LEDs).[17,19] Neither could we obtain a temperature-independent value of characteristic trap depth ($E_t=kT_t$). In LEDs, bulk-dominated current flow involves all the molecules, which are identical in nature. In contrast, in the high state of an electrically bistable device, only some of the molecules are reduced till channels of percolating networks are formed for current transport. Such morphology of the device in its high-conducting state might have led to a low value of m.

In conclusion, we have observed electrical bistability at different temperatures (10–300 K). We have studied transport mechanism of a bistable device in its two conducting states. We have shown that injection-dominated conduction mechanism determined the current in the low-conducting state. In the high state, space-charge limited conduction process with an exponential distribution of traps fitted the I-V characteristics. From the temperature dependence of electrical bistability, we found that the threshold voltage of switching increases with a decrease in temperature. The bistability, which was associated with a memory phenomenon, displayed ROM and RAM applications.

Two of the authors (A.K.R. and S.S.) acknowledge CSIR JRF. DST, Government of India financially supported the work through Projects Nos. SP/S2/M-44/99 and SR/S2/RFCMP-02/2005.

[1] R. S. Potember, T. O. Poehler, and D. O. Cowan, Appl. Phys. Lett. **34**, 405 (1979).
[2] K. S. Kwok and J. C. Scott, Mater. Today **5**, 28 (2002).
[3] L. P. Ma, J. Liu, and Y. Yang, Appl. Phys. Lett. **80**, 2997 (2002).
[4] A. Bandhopadhyay and A. J. Pal, J. Phys. Chem. B **107**, 2531 (2003).
[5] J. Campbell Scott, Science **304**, 62 (2004).
[6] Y. Yang, L. Ma, and J. Wu, MRS Bull. **29**, 833 (2004).
[7] Z. J. Donhauser, B. A. Mantooth, K. F. Kelly, L. A. Bumm, J. D. Monnell, J. J. Stapleton, D. W. Price, Jr., A. M. Rawlett, D. L. Allara, J. M. Tour, and P. S. Weiss, Science **292**, 2303 (2001).
[8] A. Bandyopadhyay and A. J. Pal, Appl. Phys. Lett. **84**, 999 (2004).
[9] J. Chen, M. A. Reed, A. M. Rawlett, and J. M. Tour, Science **286**, 1550 (1999).
[10] C. P. Collier, G. Mattersteig, E. W. Wong, Y. Luo, K. Beverly, J. Sampaio, F. M. Raymo, J. F. Stoddart, and J. R. Heath, Science **289**, 1172 (2000).
[11] A. O. Solak, S. Ranganathan, T. Itoh, and R. L. McCreery, Electrochem. Solid-State Lett. **5**, E43 (2002).
[12] M. Galperin, M. A. Ratner, and A. Nitzan, Nano Lett. **5**, 125 (2005).
[13] D. Ma, M. Aguiar, J. A. Freire, and I. A. Hümmelgen, Adv. Mater. (Weinheim, Ger.) **12**, 1063 (2000).
[14] L. Ma, S. Pyo, J. Ouyang, Q. Xu, and Y. Yang, Appl. Phys. Lett. **82**, 1419 (2003).
[15] S. K. Majee, A. Bandyopadhyay, and A. J. Pal, Chem. Phys. Lett. **399**, 284 (2004).
[16] R. N. Marks, D. D. C. Bradley, R. W. Jackson, P. L. Burn, and A. B. Holmes, Synth. Met. **57**, 4128 (1993).
[17] W. Brütting, S. Berleb, and A. G. Mückl, Org. Electron. **2**, 1 (2001).
[18] S. R. Forrest, P. E. Burrows, and M. E. Thompson, in *Organic Electroluminescent Materials and Devices*, edited by S. Miyata and H. S. Nalwa (Gordon and Breach, Amsterdam, 1997), p. 415.
[19] A. J. Campbell, D. D. C. Braley, and D. G. Lidzey, J. Appl. Phys. **82**, 6326 (1997).
[20] K. C. Kao and W. Hwang, in *Electrical Transport in Solids*, International Series in the Science of Solid State Vol. 14, edited by B. R. Pamplin (Pergamon, New York, 1981), pp. 64–144.
[21] A. Bandyopadhyay and A. J. Pal, J. Phys. Chem. B **109**, 6084 (2005).
[22] M. A. Lampert and P. Mark, *Current Injection in Solids* (Academic, New York, 1970).
[23] Molecular orbital calculations of the ground and excited states have been carried out with CHEM3D, CambridgeSoft Corporation, Cambridge, MA.
[24] Z. Chiguvare and V. Dyakonov, Phys. Rev. B **70**, 235207 (2004).